◆ Human Brain Mapping 35:2978–2994 (2014) ◆

Functional Connectivity Changes Differ in Early and Late-Onset Alzheimer's Disease

Natalina Gour,[1,2,3,4]* Olivier Felician,[2,3] Mira Didic,[2,3] Lejla Koric,[3] Claude Gueriot,[3] Valérie Chanoine,[1,4] Sylviane Confort-Gouny,[1,4] Maxime Guye,[1,4] Mathieu Ceccaldi,[2,3] and Jean Philippe Ranjeva[1,4]

[1]*Aix-Marseille Université, CNRS, CRMBM UMR 7339, 13385, Marseille, France*
[2]*Aix-Marseille Université, INSERM, Institut des Neurosciences des Systèmes (INS) UMR 1106, 13385, Marseille, France*
[3]*APHM, Hôpitaux de la Timone, Service de Neurologie et Neuropsychologie, 13385, Marseille, France*
[4]*APHM, Hôpitaux de la Timone, CEMEREM, 13385, Marseille, France*

Abstract: At a similar stage, patients with early onset Alzheimer's disease (EOAD) have greater neocortical but less medial temporal lobe dysfunction and atrophy than the late-onset form of the disease (LOAD). Whether the organization of neural networks also differs has never been investigated. This study aims at characterizing basal functional connectivity (FC) patterns of EOAD and LOAD in two groups of 14 patients matched for disease duration and severity, relative to age-matched controls. All subjects underwent an extensive neuropsychological assessment. Magnetic resonance imaging was used to quantify atrophy and resting-state FC focusing on : the default mode network (DMN), found impaired in earlier studies on AD, and the anterior temporal network (ATN) and dorso-lateral prefrontal network (DLPFN), respectively involved in declarative memory and executive functions. Patterns of atrophy and cognitive impairment in EOAD and LOAD were in accordance with previous reports. FC within the DMN was similarly decreased in both EOAD and LOAD relative to controls. However, a double-dissociated pattern of FC changes in ATN and DLPFN was found. EOAD exhibited decreased FC in the DLPFN and increased FC in the ATN relative to controls, while the reverse pattern was found in LOAD. In addition, ATN and DLPFN connectivity correlated respectively with memory and executive performances, suggesting that increased FC is here likely to reflect compensatory mechanisms. Thus, large-scale neural network changes in EOAD and LOAD endorse both common features and differences, probably related to a distinct distribution of pathological changes. *Hum Brain Mapp 35:2978–2994, 2014.* © 2013 Wiley Periodicals, Inc.

Key words: early onset Alzheimer disease; late onset Alzheimer disease; magnetic resonance imaging; neural networks; memory; executive function

Additional Supporting Information may be found in the online version of this article.

Contract grant sponsor: French Hospital Clinical Research Program (PHRC ADAGE, PI: M. Ceccaldi); Contract grant number: 2008-A01213-52

*Correspondence to: Natalina Gour, Centre de Resonance Magnetique Biologique et Medicale (CRMBM) AMU-CNRS 7339, Faculté de Médecine de Marseille, France. E-mail: natalina.gour@ap-hm.fr

Received for publication 19 February 2013; Revised 4 June 2013; Accepted 11 July 2013.

DOI 10.1002/hbm.22379
Published online 5 October 2013 in Wiley Online Library (wileyonlinelibrary.com).

INTRODUCTION

The concept of early onset Alzheimer's disease (EOAD) usually refers to the form of AD in which the first symptoms appear before 65 years of age. EOAD has long been opposed to the late-onset form of the disease (LOAD), or senile dementia, until they were united under the same eponym [McKhann et al., 1984] based on the fact that they share the defining neuropathological hallmarks. Although these two forms since refer to a single disease, many studies report clinical and neuroimaging differences. In particular, there is evidence that pathology does not strictly follow the stereotypical Braak staging scheme in younger patients [Braak and Braak, 1991]. On a clinical level, EOAD patients have been found with preferentially non-memory deficits in the early stages, involving language, visual or executive skills, while LOAD patients display greater memory dysfunction before other cognitive domains become impaired [Binetti et al., 1993; Jacobs et al., 1994; Imamura et al., 1998; Kalpouzos et al., 2005; Smits et al., 2012]. Also, neuroimaging studies report greater structural damage as well as metabolic and perfusion deficits in neocortical regions in EOAD, while gray matter loss and metabolic change predominates in medial temporal structures in LOAD [Kemp et al., 2003; Frisoni et al., 2005; Kalpouzos et al., 2005; Kim et al., 2005; Frisoni et al., 2007; Canu et al., 2012; Ossenkoppele et al., 2012]. Taken together, these findings suggest that the topographic distributions of pathological changes differ in EOAD and LOAD. Thus, the organization of neural networks should also differ, but this aspect has not been formally investigated yet.

Over the past decade, a large number of studies have attempted to characterize neural networks using functional activation paradigms and, more recently, basal functional connectivity during resting state. This approach allows delineating several well-recognized and reproducible resting-state networks thought to reflect anatomo-functional systems [Greicius et al., 2003; Varoquaux et al., 2010]. In addition, recent studies support the proposal that neurodegenerative diseases are not diffuse but target selective vulnerable neural networks [Didic et al., 1999; Seeley et al., 2009; Pievani et al., 2011; Greicius and Kimmel, 2012]. In AD, several groups have reported changes in the pattern of connectivity concerning the default mode network, particularly in its posterior part, and the interconnected medial temporal structures [Li et al., 2002; Greicius et al., 2004; Rombouts et al., 2005; Wang et al., 2006; Allen et al., 2007; He et al., 2007; Bai et al., 2009; Agosta et al., 2012; Brier et al., 2012; Morbelli et al., 2012]. There is recent evidence that other cognitive networks, such as the antero-medial temporal and executive control networks are impaired in the early stages of AD [Gour et al., 2011; Agosta et al., 2012; Brier et al., 2012].

The present study aims at characterizing neuropsychological features, structural changes and basal functional connectivity (FC) patterns in EOAD and LOAD patients relative to matched control subjects. We focused on three networks, in which connectivity has been found altered in AD in earlier studies (i) the default mode network (DMN) [Greicius et al., 2004]; (ii) the antero-medial temporal network (ATN) [Kahn et al., 2008; Libby et al., 2012], involved in some aspects of declarative memory [Gour et al., 2011]; (iii) and the dorso-lateral prefrontal network (DLPFN) also named executive-control network [Seeley et al., 2007, 2009; Agosta et al., 2012; Brier et al., 2012]. Relationships between FC of these networks and neuropsychological performance were also investigated.

MATERIAL AND METHODS

Subjects

Patients were recruited at the memory clinic of the department of Neurology and Neuropsychology, Timone Hospital, Marseille. As part of the routine assessment, all patients underwent a neurological examination, a neuropsychological evaluation, a brain MRI and usual laboratory workup to rule out nondegenerative causes of cognitive impairment. The diagnosis of probable AD was consensually established by trained neurologists and neuropsychologists according to past and recent recommendations [McKhann et al., 1984, 2011]. Age at onset was estimated during a structured interview of the patient and caregiver. To obtain a relevant comparison between early and late-onset forms of the disease, only patients with a typical (amnestic) presentation at onset were selected. In addition, given the possibility of misdiagnosis in early and late-onset dementia [Barkhof et al., 2007; Dawe et al., 2011; Middleton et al., 2011; Snowden et al., 2011], only patients with probable AD with a high level of evidence for a pathophysiological process related to AD were included, that is, clinical criteria for probable AD and biomarkers demonstrating evidence of both amyloïdopathy and neuronal injury [McKhann et al., 2011]. Cerebro Spinal Fluid (CSF) analysis was thus performed in all patients prior to inclusion. CSF was subjected to the usual workup (cell counts, total protein levels, CSF/serum albumin ratio and oligoclonal bands). Total Tau, P-Tau 181 and Aβ42 peptide levels were determined using ELISA, the Innotest-hTau-Ag-kit, the Innotest Phospho-Tau (181P) kit and the Innotest Aβ42 kit respectively (Innogenetics, Ghent, Belgium).

Clinical inclusion criteria were probable "amnestic" AD with high level of evidence of AD pathophysiological process, defined here by Innotest Amyloid Tau Index (IATI) < 0.8 and P-Tau > 60 (an optimal combination of CSF biomarkers that predicts AD with a specificity of 95% and a sensitivity of 85%) [Vanderstichele et al., 2006]; presence of a reliable informant; mild severity of dementia (Clinical Dementia Rating Scale (CDR) of 1) [Morris, 1993]; onset of symptoms ranging from 1 to 5 years prior to inclusion; no personal history of neurological or psychiatric disorder; no family history of AD that could suggest an

TABLE I. Demographic and neurological data

	EOAD patients	Young controls	EOAD vs. controls (*P* value)	LOAD patients	Old controls	LOAD vs. controls (*P* value)	EOAD vs. LOAD (*P* value)
N	14	14		14	14		
Age	60.3 (5.6)	59.4 (6.4)	0.7	75.1 (2.9)	72.8 (3)	0.085	0.57
Education, years	10.6 (3.7)	13.3 (3.4)	0.03	10.6 (4.3)	11.1 (3)	0.72	0.23
Gender, females/males	5/9	9/5	0.257	8/6	10/4	0.69	0.45
Handeness	14/0	14/0		14/0	12/2		
Right/left							
CDR	1	0		1	0		
MMSE	18.9 (4.2)	29.3 (0.9)	0.0001	21.5 (3.2)	29.4 (0.5)	0.0001	0.1
Disease duration, years	2.93 (1.2)			2.79 (1.05)			
APOE							0.24
E4 homozygote	$N = 2$	None		None	None		
E4 heterozygote	$N = 8$	None		$N = 7$	$N = 1$		
IATI	0.54 (0.44)			0.41 (0.21)			0.41
Phospho-Tau 181	114.07 (32.2)			99.54 (41.03)			0.23
Amyloid	416.4 (83)			342 (128.9)			0.18

Values denote mean (standard deviation) or number. Group effects were analyzed using t-test for continuous variables and χ^2 test for dichotomous variables, p value denotes statistical significance. EOAD: Early Onset Alzheimer's Disease; LOAD: Late-Onset Alzheimer's Disease; CDR: Clinical Dementia Rating; MMSE: Mini-Mental State Examination; IATI: Innotest Amyloid Tau Index derived from CSF analysis

autosomal dominant inheritance; no abnormal feature on brain MRI including stroke, more than one ischemic lacuna, and white matter changes on FLAIR, above grade 2 at the Fazekas scale [Fazekas et al., 1987].

The cut-off of 65 years of age at onset used to classify the two subgroups of AD patients was chosen according to previous reports, primarily established on clinical grounds [Amaducci et al., 1986], and then used in most studies comparing features of early onset versus late-onset AD patients [Kemp et al., 2003; Kim et al., 2005; Shiino et al., 2006; Frisoni et al., 2007; Rabinovici et al., 2010; Canu et al., 2012; Sa et al., 2012; Smits et al., 2012; Cho et al., 2013]. This cut-off is also used in the DSM-IV TR nomenclature to specify subtypes [American Psychiatric Association, 2000].

Indeed, fourteen consecutively recruited EOAD and fourteen LOAD patients were included (CDR = 1; MMSE EOAD = 19 ± 4.2; MMSE LOAD = 21 ± 3) (EOAD age range of onset: 50–64; mean: 60.3 ± 5.6; LOAD age range of onset: 67–76; mean: 75.1 ± 3) (Table I). Two groups of fourteen healthy subjects were matched for age with the two patients groups. Controls had no history of neurological or psychiatric disorder, no cognitive complaint, normal performance on neuropsychological assessment and no abnormal feature on structural brain MRI and 18-FDG-PET imaging (CDR = 0; MMSE young controls = 29 ± 0.9; MMSE old controls = 29 ± 0.5) (Table I). All subjects provided informed consent to participate in the study, which was approved by the local Ethical Committee. Patients and healthy controls underwent a full neurological examination, a standardized neuropsychological evaluation and brain MRI which included resting state fMRI. Apo E genotype was obtained in all subjects using Hha 1 digestion and electrophoresis analysis.

Neuropsychological Assessment

All subjects underwent a comprehensive cognitive assessment. Anterograde memory was assessed using two tasks: (i) the RL/RI 16, a French version of the Free and Cued Selective Reminding test (FCSR) [Grober et al., 1988; Van Der Linden et al., 2004], which evaluates verbal memory based on the learning of a list of sixteen unrelated words; (ii) the Delayed Matching to Sample-48 items-test (DMS48), assessing visual recognition memory [Barbeau et al., 2004]. Retrograde semantic memory was assessed using the TOP 10 [Thomas-Antérion and Puel, 2006]. This standardized test evaluates biographical knowledge of 10 celebrities who have been famous between 1950 and the early 2000s.

Executive skills were assessed using four tasks: the digit forward and backward span (Wechsler Adult Intelligence Scale) [Wechsler, 2000], the forward and backward visuo-spatial span (MEM III) [Wechsler, 2001], the category and phonemic verbal fluency tasks [Cardebat, 1990] and the modified Wisconsin Card Sorting Test (WCST) [Nelson, 1976].

Visuo-perceptual skills were evaluated with the Benton Facial Recognition Test [Benton, 1994], and visuo-spatial skills with the Benton Judgment of Lines Orientation Test [Benton, 1983] and the copy of the Rey figure [Rey, 1941, 1960]. Naming was assessed using a French standardized picture naming task, the DO 80 [Deloche, 1997].

Concerning the assessment of memory, the following variables were retained for statistical analysis: total recall (free and cued) and recognition scores on the RL/RI 16, performance on delayed recognition on the DMS48, and the TOP 10 (total score). Concerning executive functions, language, visuo-perceptual and visuo-spatial skills, total raw scores were considered for analysis. Group comparisons were performed using ANOVA with two factors (JMP software): group (AD versus controls) and age (<65 years versus > 65 years).

MRI Procedures

Data acquisition

Imaging was performed on a 3T Magnetom Verio MR Scanner (Siemens, Erlangen, Germany) equipped with a 12 channel head coil. Foam padding and headphones were used to limit head motion and reduce scanner noise. Conventional MRI included 3D MPRAGE T_1-weighted images (TE/TR 2.99 ms/2,300 ms, 144 contiguous slices, 1.3 mm slice thickness, field of view (FOV) 250 mm, matrix 256) acquired in the sagittal plane. Resting-state fMRI acquisition was composed of 250 brain volumes using single-shot GE-EPI sequence (TE/TR 28 ms/3,600 ms; 50 contiguous slices, 2.5-mm thickness, matrix 122, FOV 250 mm) acquired during rest when subjects were instructed to keep their eyes closed and to stay awake with no precise thinking.

Data processing

Structural imaging. To obtain gray matter (GM) tissue probability maps and compare atrophy between the different groups of subjects, 3D T_1-weighted magnetic resonance images were postprocessed using the VBM 8 toolbox implemented of SPM8 software (Welcome Trust Centre for Neuroimaging, London, UK). Briefly, MRI data were spatially normalized (MNI space), segmented to isolate the GM partition, and modulated. The resulting images, expressed as GM volume corrected for brain size, were masked (75%) to remove remaining non-GM voxels and smoothed (FWHM 6 mm). To characterize atrophy patterns, a four-group ANOVA was performed in SPM8 (LOAD, EOAD, young controls, old controls). We first compared the two groups of patients with their age-matched controls, and then performed direct comparisons between EOAD and LOAD using an exclusive mask of regions found to differ between young and old controls. We also carried out direct GM volume comparison of EOAD versus LOAD using the age correction method of Dukart et al. [2011] (results provided in Supporting Information Fig. S2).

Functional imaging. *Preprocessing.* Preprocessing of resting-state fMRI data was conducted using a set of steps common to conventional fMRI studies. Images were corrected for acquisition delays (slice timing), realigned before spatial normalization (nonlinear registration) and smoothed (FWHM 4 mm). This was followed by a series of preprocessing steps specific to analysis functional correlations [Fox et al., 2005] which were performed using the RESTing-state fMRI data analysis toolkit (REST, by Song Xiaowei, http://resting-fmri.sourceforge.net) of SPM8. Data were detrended and temporally filtered to extract frequencies inferior to <0.08 Hz. Sources of spurious or regionally nonspecific variance related to physiological artifacts (CSF pulsations, head motions, etc.) were removed by regressing signals extracted from one region of the lateral ventricles (CSF), one region from the deep cerebral white matter and the parameters obtained by rigid body head motion correction. Comparisons of the six realignment parameters of movement between each group of subjects were performed using *t*-test. No significant difference was observed.

Seed connectivity analysis. To quantify changes of resting-state connectivity within the antero-medial temporal network (ATN), the dorso-lateral prefrontal network (DLPFN) and the default mode network (DMN), whole brain connectivity maps derived from a priori seed regions were computed. A total of five seeds (spheres with 5-mm radius) were chosen based on MNI coordinates reported in previous studies: (i) one seed in the posterior cingulate cortex (PCC) to study connectivity of the DMN based on Hedden et al. [2009] (MNI coordinates: $X = 0$, $Y = -53$, $Z = 26$); (ii) two seeds in the left and right perirhinal cortex to study connectivity of the ATN based on Kahn et al. [2008] (MNI coordinates: left seed: $X = -24$, $Y = -10$, $Z = 22$; right seed: $X = 22$, $Y = -10$, $Z = -22$); iii) and two seeds in the left and right dorsolateral prefrontal cortex (DLPFC) to study connectivity of the DLPFN based on Seeley et al. [2007] (MNI coordinates: left seed: $X = -44$, $Y = 36$, $Z = 20$; right seed: $X = 44$, $Y = 36$; $Z = 20$).

Correlation maps for each seed were computed by correlating regional time courses (averaged over all voxels within the seed region) with every voxel in the brain. Correlation maps were, then, converted to z maps using Fisher's transformation.

To characterize FC patterns, z individual maps were entered in a four-group ANOVA in SPM8 (LOAD, EOAD, young controls, old controls). To limit the impact of global GM atrophy and CSF partial volume effect on signal time courses, the proportion of GM volume was entered as a confounding covariate and one explicit GM mask (threshold 75%) was used for connectivity analyses.

Relationships between connectivity maps and neuropsychological data. Regression analyses in SPM8 were performed to study correlations between each connectivity map and neuropsychological performance in patients. To control for differences of GM volume between subjects, the proportion of GM volume was entered as a confounding covariate in analyses. Only performance on tasks that showed differences between two patients groups were entered into this analysis.

TABLE II. Neuropsychological data

		EOAD patients	Young controls	EOAD vs. Young controls (*P* value)	LOAD patients	Old controls	EOAD vs. young controls (*P* value)	Interaction (group × age) (*P* value)
Memory tests	DMS 48, delayed recall (% correct)	84.4 (13)	96 (5)	0.004	71.7 (18.3)	94.1 (7)	0.0001	0.08
	TOP 10, total score (60)	31.3 (7.9)	52.6 (4)	0.0001	17.8 (10.5)	50.8 (7.9)	0.0001	0.008
	RL/RI 16 Total free recall (48)	3.3 (3.8)	33.8 (3.63)	0.0001	3.45 (4.4)	32.1 (5.53)	0.0001	0.25
	RL/RI 16 total recall (48)	12.2 (10.9)	45 (4.56)	0.0001	14.2 (10.6)	45.3 (3)	0.0001	0.75
	RL/RI 16 recognition (48)	39.7 (5.2)	48 (0)	0.0001	38.2 (9.9)	48 (0)	0.001	0.61
Executive tests	Digit span (30)	10.4 (2.7)	14 (2.4)	0.001	11.6 (3.9)	13 (2.1)	0.27	0.145
	Spatial span (30)	7.8 (4)	16.2 (2.8)	0.0001	9.8 (3.4)	12.9 (2.2)	0.008	0.003
	WCST, criteria	2.7 (1.2)	5.9 (0.2)	0.0001	3.5 (1.8)	4.6 (1.9)	0.16	0.01
	WCST, total errors	19.4 (5.3)	4.7 (3.6)	0.0001	15.4 (6.7)	7.3 (5)	0.002	0.02
	WCST, perseverative errors	10.6 (3.6)	1.4 (2.1)	0.0001	6.5 (3.9)	2.4 (2.5)	0.004	0.005
Language, visuo-perceptual and visuo-spatial tests	Copy of Rey's figure (36)	11.6 (13.7)	34.4 (1.2)	0.0001	20.9 (13.4)	33 (4.29)	0.003	0.047
	Benton Facial Recognition Test (27)	20.6 (3)	21.5 (1)	0.263	20.3 (1.3)	24.4 (1.9)	0.09	0.95
	Benton Judgment of Lines Orientation Test (30)	14.2 (8.1)	23 (3.6)	0.001	19.1 (5.2)	21.6 (3.6)	0.17	0.03
	DO 80, naming test	71 (8.8)	80 (0)	0.001	65.3 (12.8)	79.8 (0.3)	0.0001	0.19
	Category fluency (animals)	12.8 (6.3)	29.4 (7)	0.0001	13.6 (8.6)	30.4 (6.4)	0.0001	0.97
	Alphabetic fluency (p)	13.8 (7.3)	21.6 (7.5)	0.009	14 (6.6)	18.5 (5.6)	0.06	0.36

Values denote mean (standard deviation). All performances correspond to raw scores. Numbers in brackets in the second column refer to maximum scores. Tasks were administered in the whole group of patients and controls except WCST (three missing data in EOAD and LOAD) and RL/RI 16 (three missing data in EOAD and two missing data in LOAD). Group effects were analyzed using two-factors ANOVA with factor "group" (AD vs. controls) and factor "age" (<65 years vs. > 65 years). *P* denotes statistical significance. EOAD: Early-Onset Alzheimer's Disease; LOAD: Late-Onset Alzheimer's Disease; DMS 48 = Delayed Matching to Sample-48 items-test; RL/RI 16 = French version of the free and cued selective reminding test (FCSRT); WCST: Wisconsin Card Sorting Test.

RESULTS

Demographic and Neuropsychological Data

Demographic data (Table I)

EOAD and LOAD patients did not differ from their respective control groups for age (respectively, $P = 0.708$ and $P = 0.084$, Student *t*-test) and sex (respectively, $P = 0.131$ and $P = 0.225$, χ^2 test). There was no difference between LOAD patients and age-matched controls concerning level of education ($P > 0.1$, Student *t*-test), but EOAD had received slightly less education compared with their controls (2.7 years lower on average) ($P = 0.03$, Student *t*-test). As the possibility that sex, handedness, education, APOE genotype and CSF biomarkers interact with FC could not be excluded, these variables were compared between EOAD and LOAD. There was no significant difference between the two subgroups, suggesting that patient were correctly matched on these variables.

Neuropsychological data

Both EOAD and LOAD performed significantly below age-matched controls on the MMSE and all neuropsychological variables except for the Benton Facial Recognition Test (Table II). Only LOAD did not differ from age-matched controls on the Benton Judgment of Lines Orientation and the digit span.

Interactions between group (Controls vs. Patients) and age (<65 years vs. >65 years) revealed that EOAD performed worse than LOAD patients at visuo-spatial and executive tasks, while performance was poorer on memory variables in LOAD patients. Interactions were observed for:

- performance on tasks assessing executive functions: at the spatial span ($F = 9.5$; $P = 0.003$), criteria on the Wisconsin Card Sorting Test ($F = 6.5$; $P = 0.014$), total errors ($F = 5$; $P = 0.029$) and perseverative errors ($F = 8.6$; $P = 0.005$);
- visuo-spatial functions: on the Benton Judgment of Lines Orientation Test ($F = 4.7$; $P = 0.034$) and the copy of Rey's complex figure ($F = 4.1$; $P = 0.047$);
- memory tasks, including the TOP 10 ($F = 7.5$; $P = 0.008$) and the DMS 48 ($F = 3.1$; $P = 0.08$);

No significant interaction was observed for naming and visuo-perceptual skills.

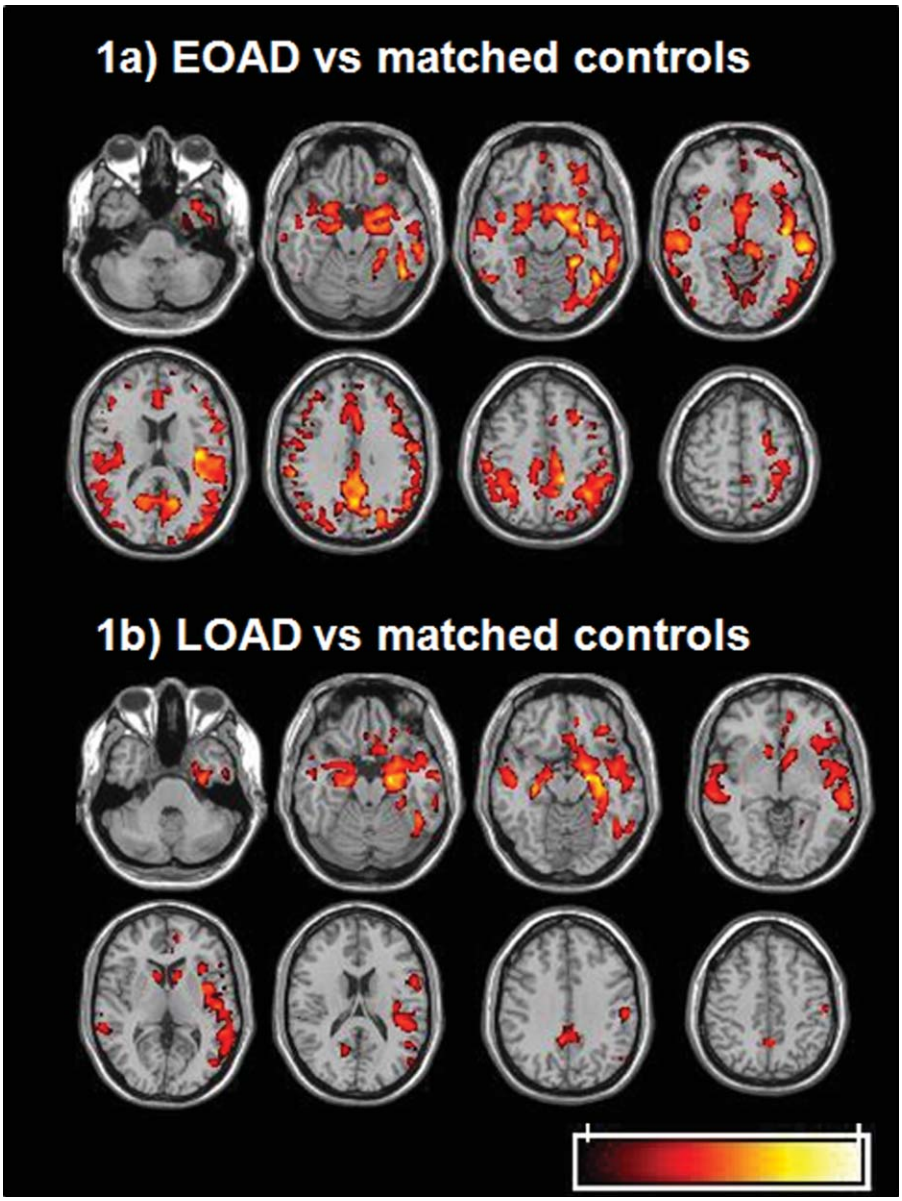

Figure 1.

Gray matter atrophy in EOAD and LOAD patients relative to age-matched controls ($P < 0.001$; $k > 10$; FDR corrected at the cluster level, $P < 0.05$) *(radiological convention: left is right)*. **a**: Gray matter loss in EOAD relative to matched controls (young). EOAD show neocortical and subcortical atrophy relative to controls that includes temporal, frontal, parietal and occipital structures along with thalamus, caudate nucleus and cerebellum. **b**: Gray matter loss in LOAD relative to matched controls (old). LOAD show atrophy in medial temporal areas (parahippocampal and hippocampal gyri and amygdala), lateral temporal structures, insula and orbito-frontal cortices relative to controls.

Atrophy

GM volumes analyses showed significant atrophy in EOAD and LOAD relative to their matched control groups (Fig. 1a,b). There was diffuse neocortical and subcortical atrophy in EOAD, while GM atrophy was more restricted to medial temporal areas, lateral temporal, insula, and orbito-frontal structures in LOAD.

When comparing EOAD and LOAD, excluding region masks showing significant differences between young and old controls to avoid the sole effect of age, more pronounced atrophy was found in the left precuneus and

posterior cingulate in EOAD relative to LOAD patients (Supporting Information Fig. S1a). By contrast, LOAD showed greater atrophy than EOAD patients in the left hippocampal and parahippocampal gyri as well as bilateral orbito-frontal regions (Supporting Information Fig. S1b).

FC Analyses

Figure 2 illustrates the five studied networks obtained in young healthy controls using seeds within the posterior cingulate for DMN, the left and right perirhinal cortices for the left and the right ATN, the left and right dorsolateral prefrontal cortices for the left and the right DLPFN respectively (see also Supporting Information data Table SI).

FC of the default mode network (DMN) derived from the posterior cingulate cortex (PCC) as seed region

EOAD versus age matched-controls. Looking at DMN connectivity map derived from the PCC as seed region, EOAD patients showed reduced connectivity of the superior, middle and medial frontal gyri (Brodmann area-BA 10, BA 11) relative to age-matched controls ($P < 0.005$, corrected for cluster extent, $P < 0.05$) (Fig. 3a, Supporting Information Table SIIa).

LOAD versus age matched-controls. In LOAD relative to age matched controls, the DMN connectivity map derived from the PCC as seed region showed also decreased connectivity of the medial frontal gyrus (BA 10, BA 11, BA 25) ($P < 0.005$, corrected for cluster extent, $P < 0.05$) (Fig. 3b, Supporting Information Table SIIa).

EOAD versus LOAD (excluding the effects of age in controls). A direct comparison showed no difference in DMN connectivity between EOAD to LOAD patients even at low threshold ($P < 0.05$, corrected for cluster extent, $P < 0.05$).

FC of the antero-medial temporal network (ATN) derived from the left and right perirhinal seeds

EOAD versus age matched-controls. Looking at ATN connectivity maps derived from the left perirhinal cortex as seed region, EOAD patients showed bilateral increases in connectivity of the inferior frontal gyrus (BA 44, BA 45), the middle and superior frontal gyri (BA 9, BA 10, BA 46), the thalamus, the caudate nucleus and the insula (BA 13) relative to age-matched controls ($P < 0.005$, corrected for cluster extent, $P < 0.05$) (Fig. 3c, Supporting Information Table SIIb). Concurrently, when comparing ATN connectivity maps derived from the right perirhinal cortex as seed region, no difference was observed between EOAD patients and age-matched controls.

LOAD versus age matched-controls. In LOAD relative to age-matched controls, ATN connectivity maps derived from the left perirhinal cortex as seed region showed increased connectivity of the right inferior frontal gyrus (BA 9, BA 44, BA 45) and the right insula (BA 13), while reduced connectivity was observed in the right lingual gyrus, the right and left calcarine sulcus, precuneus and posterior cingulate (BA 30, BA 31) ($P < 0.005$, corrected for cluster extent, $P < 0.05$) (Fig. 3d, Supporting Information Table SIIb). Comparisons of ATN connectivity maps derived from the right perirhinal cortex as seed region evidenced decreased connectivity involving bilateral occipital regions (Cuneus-BA 18) and right precuneus-posterior cingulate (BA 31) in LOAD patients relative to age-matched controls ($P < 0.005$, corrected for cluster extent, $P < 0.05$) (Fig. 3e, Supporting Information Table SIIc).

EOAD versus LOAD (excluding the effects of age in controls). When excluding region masks showing significant differences between young and old controls, the direct comparison between EOAD and LOAD patients showed subtle connectivity differences in the left ATN only observed at a low threshold of ($P < 0.05$ (corrected for cluster extent, $P < 0.05$). EOAD relative to LOAD showed bilateral increased connectivity within the insula (BA 13), the precentral gyrus, the middle and superior frontal gyri (BA 9, BA 10), cingulate (BA 23, BA 24) and anterior temporal structures (superior temporal gyrus (BA 38) and amygdala) (Supporting Information Table SIIb). Even at this low threshold of $P < 0.05$ (corrected for cluster extent, $P < 0.05$), no difference was observed between EOAD to LOAD patients for the ATN derived from the right perirhinal cortex.

FC of the dorso-lateral prefrontal network (DLPFN) derived from the left and right dorso-lateral prefrontal cortex (DLPFC) seeds

EOAD versus age-matched-controls. Relative to age-matched controls, DLPFN connectivity maps derived from the left DLPFC as seed region showed in EOAD patients reduced connectivity in the left middle occipital gyrus, cuneus, precuneus (BA 7, BA 19) and the left inferior parietal lobule ($P < 0.005$, corrected for cluster extent, $P < 0.05$) (Fig. 3f, Supporting Information Table SIId). DLPFN connectivity maps derived from the right DLPFC as seed region showed also decreased connectivity in EOAD patients relative to age-matched controls in bilateral cuneus, precuneus (BA 7, BA 19) and inferior parietal lobules (Fig. 3g, Supporting Information Table SIIe). No increase of connectivity was observed in EOAD patients ($P < 0.005$, corrected for cluster extent, $P < 0.05$).

LOAD versus age-matched-controls. In LOAD relative to age-matched controls, DLPFN connectivity maps derived from the left DLPFC as seed region showed bilateral increases in connectivity of the inferior frontal gyrus (BA 11-BA 44), precentral (BA 6) and middle cingulate (BA 32) gyri, insula (BA 13) and striatum (caudate nucleus and

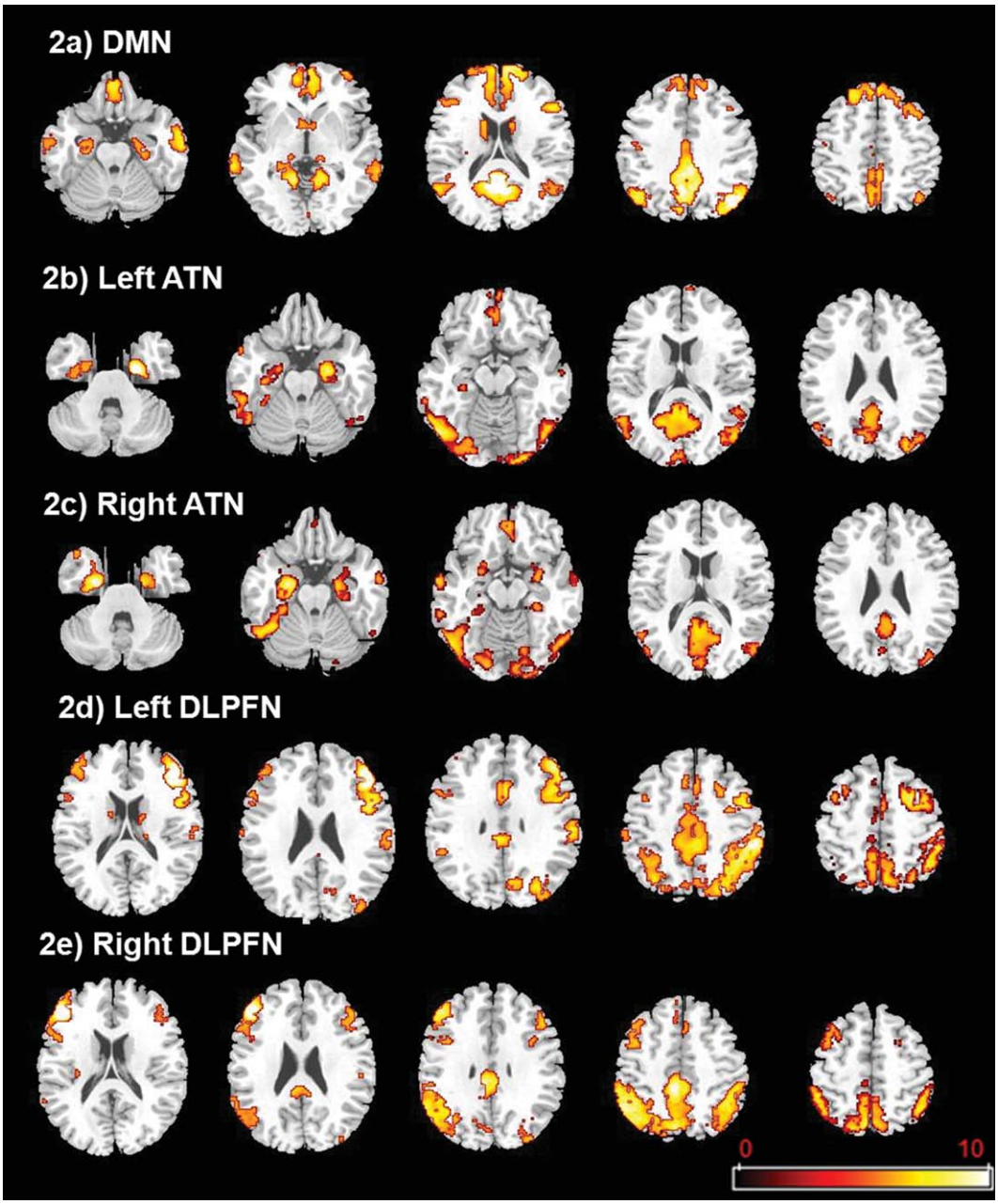

Figure 2.

Functional connectivity maps for the left and right perirhinal, left and right prefrontal and the posterior cingulate seeds in young controls ($P < 0.05$; $k > 10$; FWE corrected) *(radiological convention: left is right)*. **a**: Default-Mode Network (DMN) derived from the posterior cingulate seed. DMN includes medial and lateral prefrontal, parietal and temporal cortices. **b**: Left Antero-medial Temporal Network (ATN) derived from the left perirhinal seed. Left ATN includes bilateral medial temporal structures (anterior parahippocampal and hippocampal gyri; amygdala), lateral temporal structures, lateral and medial occipital structures, posterior cortical midline structures (precuneus and posterior cingulate) and orbito-frontal areas. **c**: Right ATN derived from the right perirhinal seed. Right ATN includes bilateral medial temporal structures (anterior parahippocampal and hippocampal gyri, amygdala), lateral temporal structures, lateral medial occipital structures, posterior cortical midline structures (precuneus and posterior cingulate) and orbito-frontal areas. **d**: Left Dorso-Lateral Pre-Frontal Network (DLPFN) derived from the left dorso-lateral prefrontal cortex seed. Left DLPFN includes bilateral lateral, medial and orbital part of frontal lobe, inferior parietal lobules and cingulate gyri. **e**: Right DLPFN derived from the right dorso-lateral prefrontal cortex seed. Right DLPFN includes bilateral lateral, medial and orbital part of frontal lobe, inferior parietal lobules and cingulate gyri.

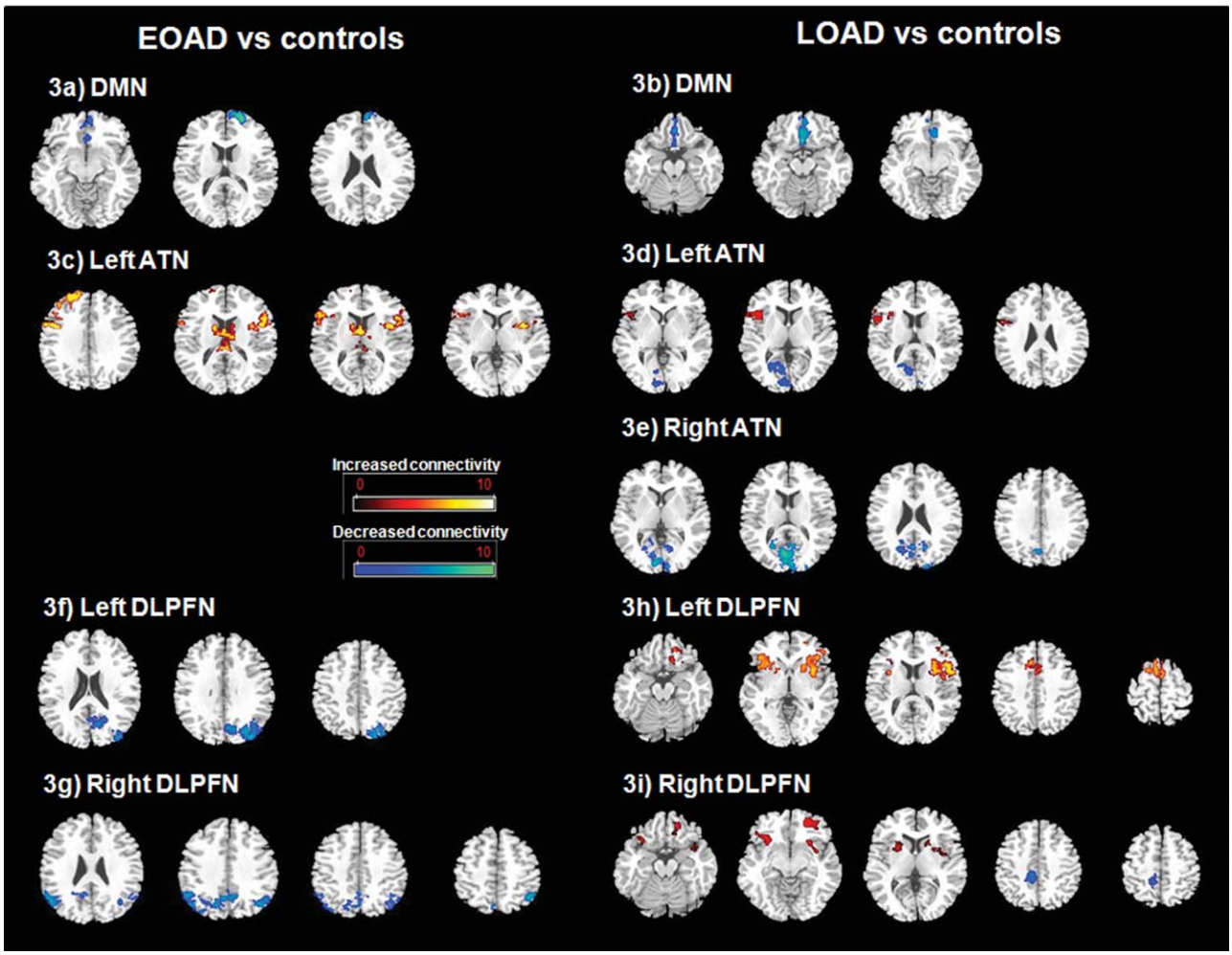

Figure 3.

Differences in resting state functional connectivity (FC) maps between EOAD and young controls (**a**; **c**; **f**; **g**), LOAD and age-matched controls (**b**; **d**; **e**; **h**; **i**) ($P < 0.005$, $k > 10$; FWE corrected at the cluster level, $P < 0.05$) *(radiological convention: left is right)*. a: Decreased FC of DMN in EOAD relative to matched controls. EOAD show decreased FC of the DMN connectivity map derived from the PCC as seed region within the superior, middle and medial frontal gyri (Brodmann area-BA 10, BA 11). b: Decreased FC of DMN in LOAD relative to matched controls. LOAD show decreased FC of the DMN connectivity map derived from the PCC as seed region within the medial frontal gyri (BA 10, BA 11, BA 25). c: Increased FC of the left ATN in EOAD relative to matched controls. EOAD show bilateral increased FC of the ATN connectivity map derived from the left perirhinal cortex as seed region within the inferior frontal gyrus (BA44, BA45), the middle and superior frontal gyri (BA 9, BA 10, BA 46), the thalamus, caudate nucleus and insula (BA 13). d: Increased (hot) and decreased (blue) FC of the left ATN in LOAD relative to matched controls. LOAD show increased FC of the ATN connectivity maps derived from the left perirhinal cortex as seed region within the right inferior frontal gyrus (BA 9, BA 44, BA 45) and the right insula (BA 13) while reduced connectivity was observed in the right lingual gyrus, the right and left calcarine sulcus and posterior cingulate (BA 30, BA 31). e: Decreased FC of the right ATN in LOAD relative to matched controls. LOAD show decreased FC of the ATN connectivity maps derived from the right perirhinal cortex as seed region within bilateral occipital regions (cuneus, BA 18) and right precuneus-posterior cingulate (BA 31). f: Decreased FC of the left DLPFN in EOAD relative to matched controls. EOAD show decreased FC of the DLPFN connectivity maps derived from the left dorso-lateral prefrontal cortex as seed region within the left middle occipital gyrus, cuneus, precuneus (BA 7, BA 19) and the left inferior parietal lobule. g: Decreased FC of the right DLPFN in EOAD relative to matched controls. EOAD show decreased FC of the DLPFN connectivity maps derived from the right dorso-lateral prefrontal cortex as seed region within bilateral cuneus, precuneus (BA7, BA 19) and inferior parietal lobules. h: Increased FC of the left DLPFN in LOAD relative to matched controls. LOAD show increased FC of the DLPFN connectivity maps derived from the left dorso-lateral prefrontal cortex as seed region within the inferior frontal gyrus (BA 11-BA 44), pre-central (BA 6) and middle cingulate (BA 32) gyri, insula (BA 13) and striatum (caudate nucleus and putamen). i: Increased (hot) and decreased (blue) FC of the right DLPFN in LOAD relative to matched controls. LOAD show increased FC of the DLPFN connectivity maps derived from the right dorso-lateral prefrontal cortex as seed region within the bilateral inferior and middle frontal gyri (BA 11, BA 47), insula and putamen while decreased FC in the precuneus/cingulate gyrus (BA 7) is observed.

putamen) ($P < 0.005$, corrected for cluster extent, $P < 0.05$) (Fig. 3h, Supporting Information Table SIId). DLPFN connectivity maps with the right DLPFC as seed region showed also increased connectivity in the bilateral inferior and middle frontal gyri (BA 11, BA 47), insula and putamen while decreased connectivity in the precuneus/cingulate gyrus (BA 7) was observed ($P < 0.005$, corrected for cluster extent, $P < 0.05$) (Fig. 3i, Supporting Information Table IIe).

EOAD versus LOAD (excluding the effects of age in controls). When excluding region masks showing significant differences between young and old controls, the direct comparison between EOAD and LOAD patients showed subtle differences in connectivity of the left DLPFN only observed at a lower threshold of ($P < 0.05$ (corrected for cluster extent, $P < 0.05$). Relative to EOAD, LOAD showed increased connectivity within the left DLPFN involving the cuneus and precuneus (BA 7, BA 19), inferior parietal lobule (BA 39, BA 40), anterior cingulate (BA 32) and precentral gyri (BA 4) and the inferior frontal and superior frontal regions (BA 6, BA 9) (Supporting Information Table IId). Even at this lower threshold ($P < 0.05$, corrected for cluster extent, $P < 0.05$), no difference was observed between EOAD to LOAD patients for the DLPFN derived from the right DLPFC.

Correlations with neuropsychological variables

Regression analyses revealed a positive correlation between connectivity of ATN derived from the left perirhinal cortex as seed region and performance on the visual recognition memory task, the DMS 48 in middle occipital gyrus, cuneus and lingual gyrus (BA 17, BA 18, BA 19, BA 23) ($P < 0.005$, corrected for cluster extent, $P < 0.05$) (Fig. 4a). Connectivity of ATN derived from the right perirhinal cortex as seed region also positively correlated with performance on the DMS 48 in the cuneus, precuneus and lingual gyrus (BA 18, BA 19, BA 30) ($P < 0.005$, corrected for cluster extent, $P < 0.05$) (Fig. 4b). Other neuropsychological measures did not significantly correlate with ATN connectivity maps.

We also observed positive correlations between DLPFN connectivity maps derived from the left DLPFC as seed region and performances on the copy of Rey's complex figure in the paracentral lobule and precuneus (BA 5 and BA 7) ($P < 0.005$, corrected for cluster extent, $P < 0.05$) (Fig. 4c). DLPFN connectivity maps derived from the right DLPFC as seed region positively correlated with performances at spatial span in inferior parietal lobule and posterior cingulate ($P < 0.005$, corrected for cluster extent, $P < 0.05$) (Fig. 4d). Other neuropsychological measures did not significantly correlate with the left and right DLPFN connectivity maps.

No significant correlation was observed between the DMN connectivity map derived from PCC as seed region and neuropsychological variables.

DISCUSSION

In this study, we examined neuropsychological, structural and FC patterns in EOAD and LOAD respectively, compared with two groups of age-matched controls. All patients had dementia of mild severity, with deficits involving memory and other cognitive domains. In accordance with previous reports, EOAD patients showed greater executive and visuo-spatial deficits while LOAD patients displayed greater memory impairment [Seltzer and Sherwin 1983; Selnes et al., 1988; Binetti et al., 1993; Jacobs et al., 1994; Koss et al., 1996; Imamura et al., 1998; Sa et al., 2012; Smits et al., 2012]. Atrophy patterns also differed between the two groups, EOAD exhibiting diffuse neocortical atrophy with greater loss in posterior cortical midline structures (precuneus, middle and posterior cingulate) while atrophy was predominant in hippocampal and orbito-frontal regions in LOAD patients, as reported in previous studies [Frisoni et al., 2005; Ishii et al., 2005; Shiino et al., 2006; Frisoni et al., 2007; Karas et al., 2007]. These behavioral and structural differences were associated with distinct patterns of FC on the large network scale. DMN connectivity was decreased to a similar extent in both patients groups. By contrast, EOAD and LOAD displayed dissociated changes of ATN and DLPFN connectivity. In EOAD patients, FC was decreased in the DLPFN but increased in the ATN, while LOAD patients exhibited decreased connectivity in posterior regions within the ATN and increased connectivity of the DLPFN. Moreover, ATN connectivity correlated with memory performance, while DLPFN connectivity correlated with performance on tasks assessing executive functions.

EOAD and LOAD Exhibit a Similar Pattern of FC Changes in the DMN

As predicted, the connectivity map derived from the posterior cingulate cortex identified the main nodes of the DMN, in particular medial and lateral prefrontal, parietal and temporal cortices [Buckner et al., 2008]. Both EOAD and LOAD groups displayed an identical pattern of decreased FC of the DMN in frontal regions, mainly in the medial prefrontal cortex, in comparison with age-matched controls. Resting-state FC of DMN has been investigated in detail in AD [Bokde et al., 2009; Sorg et al., 2009]. Our findings are consistent with previous reports on decreased FC of this network in mild AD and also in Mild Cognitive Impairment (MCI), a transitional stage between normal aging and dementia. In most of these studies, decreased connectivity was found in the posterior part of the DMN, especially in the posterior midline structures. The slightly different pattern of FC change obtained in this study is probably related to the seed region approach, here centered on the posterior cingulate. This probably significantly limits the sensitivity to evidence decreased connectivity of this seed region and neighboring ones, such as the posterior-medial structures, as usually

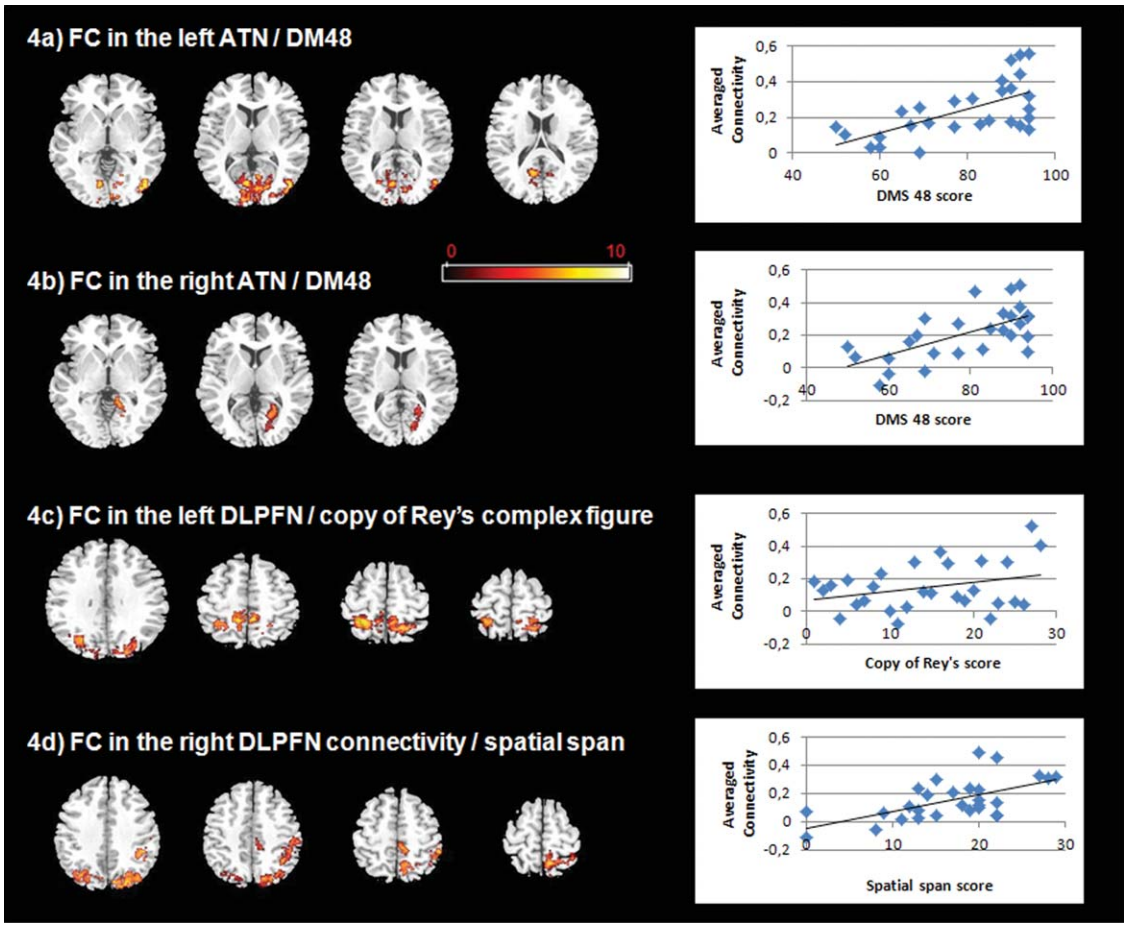

Figure 4.

Correlations between functional connectivity (FC) maps and neuropsychological variables in patients ($P < 0.005$, $k > 10$; FWE corrected at the cluster level, $P < 0.05$) *(radiological convention: left is right)*. **a**: Positive correlation between FC of left ATN and the DMS 48 (visual recognition memory task). A positive correlation between FC of left ATN and performance on the DMS 48 is observed in middle occipital gyrus, cuneus and lingual gyrus (BA 17, BA 18, BA 19, BA 23). Right side: scatter plots of averaged connectivity of significant clusters from this correlation analysis and DMS 48. **b**: Positive correlation between FC of right ATN and the DMS 48. A positive correlation between FC of right ATN and performance on the DMS 48 is observed in cuneus, precuneus and lingual gyrus (BA 18, BA 19, BA 30). Right side: scatter plots of averaged connectivity of significant clusters from this correlation analysis and DMS 48. **c**: Positive correlation between FC of left DLPFN and the copy of Rey's complex figure. A positive correlation between FC of left DLPFN and performance on the copy of Rey's complex figure is observed in paracentral lobule and precuneus (BA 5 and BA 7). Right side: scatter plots of averaged connectivity of significant clusters from this correlation analysis and Rey's complex figure. **d**: Positive correlation between FC of right DLPFN and spatial span. A positive correlation between FC of right DLPFN and performance at spatial span is observed in inferior parietal lobule and posterior cingulate. Right side: scatter plots of averaged connectivity of significant clusters from this correlation analysis and spatial span.

reported when using independent component analysis [Greicius et al., 2004; Zhou et al., 2010; Wu et al., 2011; Agosta et al., 2012; Binnewijzend et al., 2012; Damoiseaux et al., 2012].

DMN connectivity was similarly reduced in both patients groups even when lowering the threshold, and despite a highly distinctive pattern of structural changes, involving in particular the posterior part of the DMN in EOAD. This provides further evidence that DMN dysfunction does not parallel neuronal injury. It has been suggested that DMN dysfunction could be tightly linked to amyloid deposition in AD [Buckner et al., 2009]. In cognitively normal individuals amyloid accumulation correlates with functional disruption of the DMN [Hedden et al.,

2009]. Furthermore, when comparing EOAD with LOAD, no difference concerning the rate and the distribution of amyloid deposition has been found [Rabinovici et al., 2010]. Taken together, identical changes of FC within the DMN in EOAD and LOAD found in the present study could be explained by the vulnerability of this network to amyloid deposition likely to be similar in the two patients groups, both in terms of topography and severity.

In this study, no correlation between DMN resting-state connectivity and neuropsychological measures was found. As mentioned above, that decreased FC of the DMN has been found in cognitively normal individuals despite preclinical brain amyloid deposition [Hedden et al., 2009; Sheline et al., 2010] may suggest that DMN connectivity change has no specific cognitive impact. However, the DMN is primarily thought to be involved in internally focused tasks (such as autobiographical memory, prospective memory and theory of mind) and to deactivate during goal-directed tasks [Buckner et al., 2008]. Consequently, although the present findings are not in favor of a relationship between connectivity within the DMN and cognition, more specific experimental neuropsychological tasks than the ones used in the present study may be necessary to capture hypothetical cognitive consequences of DMN function and dysfunction.

Changes in FC of the ATN

The ATN was first identified by Kahn et al. [2008] in a resting-state fMRI study performed in healthy subjects using a region-of-interest method. FC change of this network, identified by ICA, has further been documented in a previous work from our group, in subjects with various memory disturbances, including subjective memory impairment, amnestic MCI and AD patients [Gour et al., 2011].

In this study, in LOAD, FC maps using the perirhinal cortices as seed regions showed decreased FC within the ATN especially in its posterior regions along with a slightly increased connectivity in the right frontal area relative to age-matched controls. These findings are consistent with the greater impairment in the realm of memory and medial temporal changes previously observed in LOAD. There is evidence that the ATN and its components are involved in specific aspects of declarative memory [Gour et al., 2011]. The present study replicates a positive correlation between ATN connectivity and performance at the DMS48, an object-based visual recognition memory task. This is coherent with evidence for the role of the perirhinal cortex and interconnected structures in object-based memory [Vargha-Khadem et al., 1997; Aggleton and Brown 1999; Eichenbaum et al., 2007; Barbeau et al., 2011] which is altered in the earliest stages of AD, as suggested by our group [Didic et al., 2011; Barbeau et al., 2012]. Taken together, these findings suggest that reduced ATN connectivity may be associated with greater memory dysfunction in LOAD.

By contrast, increased and extended connectivity of the ATN was found in EOAD, additionally involving frontoinsular regions. In resting-state fMRI studies, increased network connectivity has been observed in patients not only with mild AD but also in MCI [Wang et al., 2006, 2007; Qi et al., 2010; Zhou et al., 2010; Gour et al., 2011; Agosta et al., 2012; Das et al., 2012]. In a previous study, we observed enhanced connectivity of ATN in patients with subjective memory impairment and amnestic MCI [Gour et al., 2011]. This resting-state hyperconnectivity pattern in prefrontal regions is reminiscent of the prefrontal hyperactivation evidenced in several memory-related functional MRI studies in MCI [Heun et al., 2007] and mild AD patients [Garrido et al., 2002], traditionally interpreted as compensatory processes subsequent to medial temporal lobe pathology [Garrido et al., 2002; Guedj et al., 2009]. Hyperconnectivity observed in the present study is consistent with the compensatory account, since EOAD patients had better performance on memory tasks, and positive correlations were observed between ATN connectivity and visual recognition memory performance.

Group comparisons also revealed asymmetry in the pattern of FC changes of ATN in EAOD relative to age-matched controls. Left ATN was increased in EOAD while no effect was on the right. Only few studies have addressed the question of laterality in the pattern of FC changes associated with brain diseases. Additionally, it is worth noting that ATN has primarily been described based on a lateralized left perirhinal seed [Kahn et al., 2008]. Among the plausible explanation to account for this asymmetric pattern of FC change, one possibility is to incriminate differences in network organization between left and right hemispheres [Bettus et al., 2009]. Another possibility would relate to the spreading of the pathological process itself. Hence, lateralized structural and metabolic changes have previously been documented in AD. Hypometabolism and atrophy have been found predominantly in the left hemisphere, particularly in temporal and parietal regions, in the early stage of AD [Loewenstein et al., 1989; Janke et al., 2001; Thompson et al., 2003].

Changes in FC of the DLPFN

In this study, we found a greater decreased of FC within the DLPFN in EOAD. In the left DLPFN, EOAD patients showed reduced parietal connectivity while LOAD displayed increased frontal connectivity, in comparison with age-matched controls. On the right side, both patient-groups exhibited reduced parietal connectivity relative to controls, but enhanced frontal connectivity was, again, only observed in LOAD patients.

Structural and metabolic neuroimaging studies focusing on the effect of age in AD report greater dysfunction of frontal and parietal structures in EOAD, in comparison with the late onset form of the disease [Salmon et al., 2000; Sakamoto et al., 2002; Ishii et al., 2005; Kim et al., 2005;

Karas et al., 2007]. Using FDG-PET, Kalpouzos et al. [2005] found a specific frontal and inferior parietal hypometabolism in EOAD relative to LOAD patients. They also observed positive correlations in EOAD patients between left prefrontal metabolism and performance on the Brown-Peterson task, a widely used working memory paradigm.

A large body of evidence sustains the proposition that the prefrontal regions are part of a system supporting the executive functions in the human brain [Fuster, 2001; Alvarez and Emory, 2006]. In resting-state fMRI studies, the executive fronto-parietal network was first identified by Seeley et al. [2007] using both region-of-interest and ICA methods. These authors also observed positive correlations between the parietal node of this network and performance on the Trail Making Test, a task assessing visual spatial attention and task switching processes. In the present study, positive correlations between DLPFN connectivity and executive tasks were also found. Enhanced connectivity of the DLPFN was associated with greater performance on the copy of Rey's complex figure, involving visuo-spatial and planning skills [Schwarz et al., 2009], and at the visuo-spatial span, known to assess visual working memory [Milner, 1971]. Overall, these results are consistent with the findings of the present study showing greater reduced connectivity of a fronto-parietal executive network in EOAD patients, with a behavioral impact on executive functioning.

LOAD exhibited an increased connectivity of the DLPFN within the frontal component of the network. As previously mentioned, increased connectivity has been reported on multiple occasions in mild AD and MCI patients [Zhou et al., 2010; Das et al., 2012]. In this study, positive correlations between connectivity of DLPFN and performance on tasks assessing executive functions were also found, suggesting again the possibility of compensatory mechanisms aimed at improving network efficiency and behavioral performance in LOAD patients. The present findings are in agreement with a recent study showing increased FC of an executive network in AD patients relative to controls, with positive correlations between FC and performance assessing executive functions [Agosta et al., 2012].

EOAD and LOAD Exhibit Dissociated Patterns of FC Changes in ATN and DLPFN

In this study, unlike DMN, EOAD and LOAD subjects displayed dissociated profiles of ATN and DLPFN connectivity including the interplay of hypoconnectivity and hyperconnectivity patterns. These differential profiles of large scale network connectivity are likely to be underpinned by distinct distributions of pathological changes and related to markers of neuronal degeneration. The neuropathological hallmarks of AD are characterized by amyloid and tau deposition, as well as neuronal and synaptic loss. In the common late-onset form of AD, neurofibrillary tangles (NFTs), related to tau protein pathology and associated with clinical signs [Arriagada et al., 1992; Gomez-Isla et al., 1997], initially develop in the anterior subhippocampal cortex (entorhinal and perirhinal cortex) before reaching the hippocampal formation and then associative neocortical structures [Braak and Braak, 1991; Arriagada et al., 1992; Gomez-Isla et al., 1997; Delacourte et al., 1999]. Assuming that neurodegeneration and NFTs deposition occur in the same topographic distribution and consistent with this sequential scheme, LOAD patients with more severe mesio-temporal atrophy and related memory impairment, exhibited decreased ATN connectivity. By contrast, DLPFN connectivity was reduced in EOAD. In EOAD, neurodegeneration is likely not to strictly follow the stereotypical Braak and Braak scenario, with an earlier neocortical involvement, as suggested by previous neuroimaging studies [Kemp et al., 2003; Kalpouzos et al., 2005; Kim et al., 2005; Frisoni et al., 2007; Canu et al., 2012; Ossenkoppele et al., 2012]. Consequently, the dissociated pattern of FC change within two large scale neuronal networks, respectively associated with memory and executive functions, could be related to a distinct topography of tau-related neuronal injury in EOAD and LOAD.

Limitations of this Study

The use of a dichotomous age cut-off is a quite arbitrary conceptual construct that involves limitations especially considering the relatively small number of subjects in each subgroup of our study. In a recent multicenter study including 2000 AD patients, the cut-off of 66 of age was found to best discriminate EOAD from LOAD on a series of demographical and clinical variables [Spalletta, 2013]. However, when applying this cut-off instead of 65 to our patients' population, composition of the two subgroups remained unchanged. Additionally, age at onset is an estimate and the attempt to dichotomize the age of onset distribution is likely to introduce misclassification of subjects. Although the present findings add to the evidence that age is a factor that contributes to heterogeneity in AD, it is important to mention that several other genetic and environmental factors like APO E genotype and cognitive reserve also contribute to this heterogeneity and interact with age of onset [Katzman, 1993; Stern, 2002; van der Flier et al., 2011].

As most clinical-radiological studies performed in AD, another potential limitation is the lack of postmortem data, so the possibility of misdiagnosis cannot be excluded. Nevertheless, an extensive work-up was performed in all subjects and all patients fulfilled clinical criteria of probable AD. Furthermore, CSF biomarkers were available for each patient and supported evidence of AD pathological changes [McKhann et al., 2011]. Additionally, pathophysiological process of AD probably begins many years before clinical symptoms are apparent. Thus, the possibility that some controls do have preclinical AD cannot be formally

ruled out. But impact on data should be minimal considering the highly selective inclusion process specified above.

CONCLUSION

The present study highlights common features but also differences in organization of functional neural networks in two subtypes of AD depending on different ages at onset. A similar impairment of FC in the DMN was found in both groups. By contrast, dissociated patterns of hypo- and hyperconnectivity were observed in EOAD and LOAD, relative to age-matched controls, in two large-scale neural networks associated with memory and executive functions. These differences, which parallel behavioral and structural changes, are possibly related to distinct topographies of neuronal degeneration in EOAD and LOAD.

ACKNOWLEDGMENTS

None of the authors have any actual or potential conflicts of interest. The authors are thankful to the patients, their families and healthy controls for their generous participation in this study. They are grateful to Dr Radka Gantcheva for clinical assessment of healthy subjects, Dr Raphaelle Bernard for performing Apo E genotyping, Julie Pelat, Maryline Blanchon for their help with management of throughout the study including data managing, Mohamed Fattalah (Centre d'Investigation Clinique) for computational assistance, and Elisabeth Soulier and Patrick Viout for the MRI acquisitions. They thank Celia Rousseau and Sophie Achard to their help in movement parameters analyses. Finally, they are indebted to the association "dechaine ton coeur" for its financial support.

REFERENCES

Aggleton JP, Brown MW (1999): Episodic memory, amnesia, and the hippocampal-anterior thalamic axis. Behav Brain Sci 22: 425–444.

Agosta F, Pievani M, Geroldi C, Copetti M, Frisoni GB, Filippi M (2012): Resting state fMRI in Alzheimer's disease: Beyond the default mode network. Neurobiol Aging 33:1564–1578.

Allen G, Barnard H, McColl R, Hester AL, Fields JA, Weiner MF, Ringe WK, Lipton AM, Brooker M, McDonald E, Rubin CD, Cullum CM (2007): Reduced hippocampal functional connectivity in Alzheimer disease. Arch Neurol 64:1482–1487.

Alvarez JA, Emory E (2006): Executive function and the frontal lobes: A meta-analytic review. Neuropsychol Rev 16:17–42.

Amaducci LA, Rocca WA, Schoenberg BS (1986): Origin of the distinction between Alzheimer's disease and senile dementia: How history can clarify nosology. Neurology 36:1497–1499.

American Psychiatric association. Diagnostic and Statistical Manual Of Mental Disorders. Fourth Edition? Washington, C, American Psychiatric Asssociation, 2000.

Arriagada PV, Growdon JH, Hedley-Whyte ET, Hyman BT (1992): Neurofibrillary tangles but not senile plaques parallel duration and severity of Alzheimer's disease. Neurology 42(3 Pt 1):631–639.

Bai F, Zhang Z, Watson DR, Yu H, Shi Y, Yuan Y, Zang Y, Zhu C, Qian Y (2009): Abnormal functional connectivity of hippocampus during episodic memory retrieval processing network in amnestic mild cognitive impairment. Biol Psychiatry 65:951–958.

Barbeau E, Tramoni E, Joubert S, Mancini J, Ceccaldi M, Poncet M (2004): Évaluation de la mémoire de reconnaissance visuelle: Normalisation d'une nouvelle épreuve en choix forcé et utilité en neuropsychologie clinique. In Les troubles de la mémoire dans la maladie d'Alzheimer. Solal, Marseille. pp 85–101.

Barbeau EJ, Didic M, Joubert S, Guedj E, Koric L, Felician O, Ranjeva JP, Cozzone P, Ceccaldi M (2012): Extent and neural basis of semantic memory impairment in mild cognitive impairment. J Alzheimers Dis 28:823–837.

Barbeau EJ, Pariente J, Felician O, Puel M (2011): Visual recognition memory: A double anatomo-functional dissociation. Hippocampus 21:929–934.

Barkhof F, Polvikoski TM, van Straaten EC, Kalaria RN, Sulkava R, Aronen HJ, Niinisto L, Rastas S, Oinas M, Scheltens P, Erkinjuntti T (2007): The significance of medial temporal lobe atrophy: A postmortem MRI study in the very old. Neurology 69:1521–1527.

Benton A, Sivan AB, Hamsher KS, Varney NR, Spreen O (1994): Contributions to Neuropsychological Assessment, 2nd ed. New York.

Benton AL, Sivan AB, Hamsher KDS, Varney NR, Spreen O (1983): Contribution to Neuropsychological Assessment. New York.

Bettus G, Guedj E, Joyeux F, Confort-Gouny S, Soulier E, Laguitton V, Cozzone PJ, Chauvel P, Ranjeva JP, Bartolomei F, Guye M (2009): Decreased basal fMRI functional connectivity in epileptogenic networks and contralateral compensatory mechanisms. Hum Brain Mapp 30:1580–1591.

Binetti G, Magni E, Padovani A, Cappa SF, Bianchetti A, Trabucchi M (1993): Neuropsychological heterogeneity in mild Alzheimer's disease. Dementia 4:321–326.

Binnewijzend MA, Schoonheim MM, Sanz-Arigita E, Wink AM, van der Flier WM, Tolboom N, Adriaanse SM, Damoiseaux JS, Scheltens P, van Berckel BN, Barkhof F (2012): Resting-state fMRI changes in Alzheimer's disease and mild cognitive impairment. Neurobiol Aging 33:2018–2028.

Bokde AL, Ewers M, Hampel H (2009): Assessing neuronal networks: Understanding Alzheimer's disease. Prog Neurobiol 89: 125–133.

Braak H, Braak E (1991): Demonstration of amyloid deposits and neurofibrillary changes in whole brain sections. Brain Pathol 1: 213–216.

Brier MR, Thomas JB, Snyder AZ, Benzinger TL, Zhang D, Raichle ME, Holtzman DM, Morris JC, Ances BM (2012): Loss of intranetwork and internetwork resting state functional connections with Alzheimer's disease progression. J Neurosci 32: 8890–8899.

Buckner RL, Andrews-Hanna JR, Schacter DL (2008): The brain's default network: Anatomy, function, and relevance to disease. Ann N Y Acad Sci 1124:1–38.

Buckner RL, Sepulcre J, Talukdar T, Krienen FM, Liu H, Hedden T, Andrews-Hanna JR, Sperling RA, Johnson KA (2009): Cortical hubs revealed by intrinsic functional connectivity: mapping, assessment of stability, and relation to Alzheimer's disease. J Neurosci 29:1860–1873.

Canu E, Frisoni GB, Agosta F, Pievani M, Bonetti M, Filippi M (2012): Early and late onset Alzheimer's disease patients have

distinct patterns of white matter damage. Neurobiol Aging 33: 1023–1033.

Cardebat D, Doyon B, Puel M, Goulet P, Joanette, Y (1990): Formal and semantic lexical evocation in normal subjects. Performance and dynamics of production as a function of sex, age and educational level. Acta Neurol Belg 90:207–217.

Cho H, Seo SW, Kim JH, Kim C, Ye BS, Kim GH, Noh Y, Kim HJ, Yoon CW, Seong JK, Kim CH, Kang SJ, Chin J, Kim ST, ee KH, Na DL (2013): Changes in subcortical structures in early- versus late-onset Alzheimer's disease. Neurobiol Aging 34: 1740–1747.

Damoiseaux JS, Prater KE, Miller BL, Greicius MD (2012): Functional connectivity tracks clinical deterioration in Alzheimer's disease. Neurobiol Aging 33:828 e19–e30.

Das SR, Pluta J, Mancuso L, Kliot D, Orozco S, Dickerson BC, Yushkevich PA, Wolk DA (2012): Increased functional connectivity within medial temporal lobe in mild cognitive impairment. Hippocampus 23:1–6.

Dawe RJ, Bennett DA, Schneider JA, Arfanakis K (2011): Neuropathologic correlates of hippocampal atrophy in the elderly: A clinical, pathologic, postmortem MRI study. PLoS One 6: e26286.

Delacourte A, David JP, Sergeant N, Buee L, Wattez A, Vermersch P, Ghozali F, Fallet-Bianco C, Pasquier F, Lebert F, Petit H, Di Menza C (1999): The biochemical pathway of neurofibrillary degeneration in aging and Alzheimer's disease. Neurology 52: 1158–1165.

Deloche G, Hannequin D (1997): DO 80: épreuve de dénomination orale d'images. Paris.

Didic M, Barbeau EJ, Felician O, Tramoni E, Guedj E, Poncet M, Ceccaldi M (2011): Which memory system is impaired first in Alzheimer's disease? J Alzheimers Dis 27:11–22.

Didic M, Felician O, Ceccaldi M, Poncet M (1999): Progressive focal cortical atrophies. Rev Neurol (Paris) 155 Suppl 4:S73–S82.

Dukart J, Schroeter ML, Mueller K (2011): Age correction in dementia—Matching to a healthy brain. PLoS One 6:e22193.

Eichenbaum H, Yonelinas AP, Ranganath C (2007): The medial temporal lobe and recognition memory. Annu Rev Neurosci 30:123–152.

Fazekas F, Chawluk JB, Alavi A, Hurtig HI, Zimmerman RA (1987): MR signal abnormalities at 1.5 T in Alzheimer's dementia and normal aging. AJR Am J Roentgenol 149:351–356.

Fox MD, Snyder AZ, Vincent JL, Corbetta M, Van Essen DC, Raichle ME (2005): The human brain is intrinsically organized into dynamic, anticorrelated functional networks. Proc Natl Acad Sci USA 102:9673–9678.

Frisoni GB, Pievani M, Testa C, Sabattoli F, Bresciani L, Bonetti M, Beltramello A, Hayashi KM, Toga AW, Thompson PM (2007): The topography of grey matter involvement in early and late onset Alzheimer's disease. Brain 130(Pt 3):720–730.

Frisoni GB, Testa C, Sabattoli F, Beltramello A, Soininen H, Laakso MP (2005): Structural correlates of early and late onset Alzheimer's disease: Voxel based morphometric study. J Neurol Neurosurg Psychiatry 76:112–114.

Fuster JM (2001): The prefrontal cortex—An update. Time is of the essence. Neuron 30:319–333.

Garrido GE, Furuie SS, Buchpiguel CA, Bottino CM, Almeida OP, Cid CG, Camargo CH, Castro CC, Glabus MF, Busatto GF (2002): Relation between medial temporal atrophy and functional brain activity during memory processing in Alzheimer's disease: A combined MRI and SPECT study. J Neurol Neurosurg Psychiatry 73:508–516.

Gomez-Isla T, Hollister R, West H, Mui S, Growdon JH, Petersen RC, Parisi JE, Hyman BT (1997): Neuronal loss correlates with but exceeds neurofibrillary tangles in Alzheimer's disease. Ann Neurol 41:17–24.

Gour N, Ranjeva JP, Ceccaldi M, Confort-Gouny S, Barbeau E, Soulier E, Guye M, Didic M, Felician O (2011): Basal functional connectivity within the anterior temporal network is associated with performance on declarative memory tasks. Neuroimage 58:687–697.

Greicius MD, Kimmel DL (2012): Neuroimaging insights into network-based neurodegeneration. Curr Opin Neurol 25:727–734.

Greicius MD, Krasnow B, Reiss AL, Menon V (2003): Functional connectivity in the resting brain: A network analysis of the default mode hypothesis. Proc Natl Acad Sci USA 100:253–258.

Greicius MD, Srivastava G, Reiss AL, Menon V (2004): Default-mode network activity distinguishes Alzheimer's disease from healthy aging: Evidence from functional MRI. Proc Natl Acad Sci USA 101:4637–4642.

Grober E, Buschke H, Crystal H, Bang S, Dresner R (1988): Screening for dementia by memory testing. Neurology 38:900–903.

Guedj E, Barbeau EJ, Didic M, Felician O, de Laforte C, Ranjeva JP, Poncet M, Cozzone PJ, Mundler O, Ceccaldi M (2009): Effects of medial temporal lobe degeneration on brain perfusion in amnestic MCI of AD type: Deafferentation and functional compensation? Eur J Nucl Med Mol Imaging 36:1101–1112.

He Y, Wang L, Zang Y, Tian L, Zhang X, Li K, Jiang T (2007): Regional coherence changes in the early stages of Alzheimer's disease: A combined structural and resting-state functional MRI study. Neuroimage 35:488–500.

Hedden T, Van Dijk KR, Becker JA, Mehta A, Sperling RA, Johnson KA, Buckner RL (2009): Disruption of functional connectivity in clinically normal older adults harboring amyloid burden. J Neurosci 29:12686–12694.

Heun R, Freymann K, Erb M, Leube DT, Jessen F, Kircher TT, Grodd W (2007): Mild cognitive impairment (MCI) and actual retrieval performance affect cerebral activation in the elderly. Neurobiol Aging 28:404–413.

Imamura T, Takatsuki Y, Fujimori M, Hirono N, Ikejiri Y, Shimomura T, Hashimoto M, Yamashita H, Mori E (1998): Age at onset and language disturbances in Alzheimer's disease. Neuropsychologia 36:945–949.

Ishii K, Kawachi T, Sasaki H, Kono AK, Fukuda T, Kojima Y, Mori E (2005): Voxel-based morphometric comparison between early- and late-onset mild Alzheimer's disease and assessment of diagnostic performance of z score images. AJNR Am J Neuroradiol 26:333–340.

Jacobs D, Sano M, Marder K, Bell K, Bylsma F, Lafleche G, Albert M, Brandt J, Stern Y (1994): Age at onset of Alzheimer's disease: Relation to pattern of cognitive dysfunction and rate of decline. Neurology 44:1215–1220.

Janke AL, de Zubicaray G, Rose SE, Griffin M, Chalk JB, Galloway GJ (2001): 4D deformation modeling of cortical disease progression in Alzheimer's dementia. Magn Reson Med 46:661–666.

Kahn I, Andrews-Hanna JR, Vincent JL, Snyder AZ, Buckner RL (2008): Distinct cortical anatomy linked to subregions of the medial temporal lobe revealed by intrinsic functional connectivity. J Neurophysiol 100:129–139.

Kalpouzos G, Eustache F, de la Sayette V, Viader F, Chetelat G, Desgranges B (2005): Working memory and FDG-PET dissociate early and late onset Alzheimer disease patients. J Neurol 252:548–558.

Karas G, Scheltens P, Rombouts S, van Schijndel R, Klein M, Jones B, van der Flier W, Vrenken H, Barkhof F (2007): Precuneus atrophy in early-onset Alzheimer's disease: A morphometric structural MRI study. Neuroradiology 49:967–976.

Katzman R (1993): Education and the prevalence of dementia and Alzheimer's disease. Neurology 43:13–20.

Kemp PM, Holmes C, Hoffmann SM, Bolt L, Holmes R, Rowden J, Fleming JS (2003): Alzheimer's disease: Differences in technetium-99m HMPAO SPECT scan findings between early onset and late onset dementia. J Neurol Neurosurg Psychiatry 74:715–719.

Kim EJ, Cho SS, Jeong Y, Park KC, Kang SJ, Kang E, Kim SE, Lee KH, Na DL (2005): Glucose metabolism in early onset versus late onset Alzheimer's disease: An SPM analysis of 120 patients. Brain 128(Pt 8):1790–1801.

Koss E, Edland S, Fillenbaum G, Mohs R, Clark C, Galasko D, Morris JC (1996): Clinical and neuropsychological differences between patients with earlier and later onset of Alzheimer's disease: A CERAD analysis, Part XII. Neurology 46:136–141.

Li SJ, Li Z, Wu G, Zhang MJ, Franczak M, Antuono PG (2002): Alzheimer Disease: Evaluation of a functional MR imaging index as a marker. Radiology 225:253–259.

Libby LA, Ekstrom AD, Ragland JD, Ranganath C (2012): Differential connectivity of perirhinal and parahippocampal cortices within human hippocampal subregions revealed by high-resolution functional imaging. J Neurosci 32:6550–6560.

Loewenstein DA, Barker WW, Chang JY, Apicella A, Yoshii F, Kothari P, Levin B, Duara R (1989): Predominant left hemisphere metabolic dysfunction in dementia. Arch Neurol 46: 146–152.

McKhann G, Drachman D, Folstein M, Katzman R, Price D, Stadlan EM (1984): Clinical diagnosis of Alzheimer's disease: Report of the NINCDS-ADRDA Work Group under the auspices of Department of Health and Human Services Task Force on Alzheimer's Disease. Neurology 34:939–944.

McKhann GM, Knopman DS, Chertkow H, Hyman BT, Jack CR Jr, Kawas CH, Klunk WE, Koroshetz WJ, Manly JJ, Mayeux R, Mohs RC, Morris JC, Rossor MN, Scheltens P, Carrillo MC, Thies B, Weintraub S, Phelps CH (2011): The diagnosis of dementia due to Alzheimer's disease: Recommendations from the National Institute on Aging-Alzheimer's Association workgroups on diagnostic guidelines for Alzheimer's disease. Alzheimers Dement 7:263–269.

Middleton LE, Grinberg LT, Miller B, Kawas C, Yaffe K (2011): Neuropathologic features associated with Alzheimer disease diagnosis: Age matters. Neurology 77:1737–1744.

Milner B (1971): Interhemispheric differences in the localization of psychological processes in man. Br Med Bull 27:272–277.

Morbelli S, Drzezga A, Perneczky R, Frisoni GB, Caroli A, van Berckel BN, Ossenkoppele R, Guedj E, Didic M, Brugnolo A, Sambuceti G, Pagani M, Salmon E, Nobili F (2012): Resting metabolic connectivity in prodromal Alzheimer's disease. A European Alzheimer Disease Consortium (EADC) project. Neurobiol Aging 33:2533–2550.

Morris JC (1993): The Clinical Dementia Rating (CDR): Current version and scoring rules. Neurology 43:2412–2414.

Nelson HE (1976): A modified card sorting test sensitive to frontal lobe defects. Cortex 12:313–324.

Ossenkoppele R, Zwan MD, Tolboom N, van Assema DM, Adriaanse SF, Kloet RW, Boellaard R, Windhorst AD, Barkhof F, Lammertsma AA, Scheltens P, van der Flier WM, van Berckel BN (2012): Amyloid burden and metabolic function in early-onset Alzheimer's disease: Parietal lobe involvement. Brain 135(Pt 7):2115–2125.

Pievani M, de Haan W, Wu T, Seeley WW, Frisoni GB (2011): Functional network disruption in the degenerative dementias. Lancet Neurol 10:829–843.

Qi Z, Wu X, Wang Z, Zhang N, Dong H, Yao L, Li K (2010): Impairment and compensation coexist in amnestic MCI default mode network. Neuroimage 50:48–55.

Rabinovici GD, Furst AJ, Alkalay A, Racine CA, O'Neil JP, Janabi M, Baker SL, Agarwal N, Bonasera SJ, Mormino EC, Weiner MW, Gorno-Tempini ML, Rosen HJ, Miller BL, Jagust WJ (2010): Increased metabolic vulnerability in early-onset Alzheimer's disease is not related to amyloid burden. Brain 133(Pt 2): 512–528.

Rey A (1941): "L'examen psychologique dans les cas d'encephalopathie traumatique. Arch Psychol 28:215–285.

Rey A (1960): Test de la figure complexe de Rey. ECPA, Paris.

Rombouts SA, Barkhof F, Goekoop R, Stam CJ, Scheltens P (2005): Altered resting state networks in mild cognitive impairment and mild Alzheimer's disease: An fMRI study. Hum Brain Mapp 26:231–239.

Sa F, Pinto P, Cunha C, Lemos R, Letra L, Simoes M, Santana I (2012): Differences between early and late-onset alzheimer's disease in neuropsychological tests. Front Neurol 3:81.

Sakamoto S, Ishii K, Sasaki M, Hosaka K, Mori T, Matsui M, Hirono N, Mori E (2002): Differences in cerebral metabolic impairment between early and late onset types of Alzheimer's disease. J Neurol Sci 200:27–32.

Salmon E, Collette F, Degueldre C, Lemaire C, Franck G (2000): Voxel-based analysis of confounding effects of age and dementia severity on cerebral metabolism in Alzheimer's disease. Hum Brain Mapp 10:39–48.

Schwarz L, Penna S, Novack T (2009): Factors contributing to performance on the Rey Complex Figure Test in individuals with traumatic brain injury. Clin Neuropsychol 23:255–267.

Seeley WW, Crawford RK, Zhou J, Miller BL, Greicius MD (2009): Neurodegenerative diseases target large-scale human brain networks. Neuron 62:42–52.

Seeley WW, Menon V, Schatzberg AF, Keller J, Glover GH, Kenna H, Reiss AL, Greicius MD (2007): Dissociable intrinsic connectivity networks for salience processing and executive control. J Neurosci 27:2349–2356.

Selnes OA, Carson K, Rovner B, Gordon B (1988): Language dysfunction in early- and late-onset possible Alzheimer's disease. Neurology 38:1053–1056.

Seltzer B, Sherwin I (1983): A comparison of clinical features in early- and late-onset primary degenerative dementia. One entity or two? Arch Neurol 40:143–146.

Sheline YI, Raichle ME, Snyder AZ, Morris JC, Head D, Wang S, Mintun MA (2010): Amyloid plaques disrupt resting state default mode network connectivity in cognitively normal elderly. Biol Psychiatry 67:584–587.

Shiino A, Watanabe T, Maeda K, Kotani E, Akiguchi I, Matsuda M (2006): Four subgroups of Alzheimer's disease based on patterns of atrophy using VBM and a unique pattern for early onset disease. Neuroimage 33:17–26.

Smits LL, Pijnenburg YA, Koedam EL, van der Vlies AE, Reuling IE, Koene T, Teunissen CE, Scheltens P, van der Flier WM

(2012): Early onset Alzheimer's disease is associated with a distinct neuropsychological profile. J Alzheimers Dis 30:101–108.

Snowden JS, Thompson JC, Stopford CL, Richardson AM, Gerhard A, Neary D, Mann DM (2011): The clinical diagnosis of early-onset dementias: Diagnostic accuracy and clinicopathological relationships. Brain 134(Pt 9):2478–2492.

Sorg C, Riedl V, Perneczky R, Kurz A, Wohlschlager AM (2009): Impact of Alzheimer's disease on the functional connectivity of spontaneous brain activity. Curr Alzheimer Res 6:541–553.

Spalletta GDLV, Padovani A, Rozzini L, Perri R, Bruni A, Canonico V, Trequattrini A, Bellelli G, Pettenati C, Pazzelli F, Caltagirone C, Orfei MD (2013): Early onset versus late onset in Alzheimer's disease: What is the reliable cut-off? Adv Alzheimer's Dis 2:40–47.

Stern Y (2002): What is cognitive reserve? Theory and research application of the reserve concept. J Int Neuropsychol Soc 8: 448–460.

Thomas-Antérion C, Puel M (2006): La mémoire collective, mémoire des évènements publics et des célébrités: les batterie EVE 30 et TOP 30. Solal, Marseille.

Thompson PM, Hayashi KM, de Zubicaray G, Janke AL, Rose SE, Semple J, Herman D, Hong MS, Dittmer SS, Doddrell DM, Toga AW (2003): Dynamics of gray matter loss in Alzheimer's disease. J Neurosci 23:994–1005.

van der Flier WM, Pijnenburg YA, Fox NC, Scheltens P (2011): Early-onset versus late-onset Alzheimer's disease: The case of the missing APOE varepsilon4 allele. Lancet Neurol 10:280–288.

Van Der Linden M, Coyette F, Poitrenaud J (2004): L'épreuve de rappel libre/rappel indicé à 16 items (RL/RI-16). In L'évaluation des troubles de la mémoire. Marseille. Solal, pp 85–101.

Vanderstichele H, De Vreese K, Blennow K, Andreasen N, Sindic C, Ivanoiu A, Hampel H, Burger K, Parnetti L, Lanari A, Padovani A, DiLuca M, Blaser M, Olsson AO, Pottel H, Hulstaert F, Vanmechelen (2006): Analytical performance and clinical utility of the INNOTEST PHOSPHO-TAU181P assay for discrimination between Alzheimer's disease and dementia with Lewy bodies. Clin Chem Lab Med 44:1472–1480.

Vargha-Khadem F, Gadian DG, Watkins KE, Connelly A, Van Paesschen W, Mishkin M (1997): Differential effects of early hippocampal pathology on episodic and semantic memory. Science 277:376–380.

Varoquaux G, Sadaghiani S, Pinel P, Kleinschmidt A, Poline JB, Thirion B (2010): A group model for stable multi-subject ICA on fMRI datasets. Neuroimage 51:288–299.

Wang K, Liang M, Wang L, Tian L, Zhang X, Li K, Jiang T (2007): Altered functional connectivity in early Alzheimer's disease: A resting-state fMRI study. Hum Brain Mapp 28:967–978.

Wang L, Zang Y, He Y, Liang M, Zhang X, Tian L, Wu T, Jiang T, Li K (2006): Changes in hippocampal connectivity in the early stages of Alzheimer's disease: Evidence from resting state fMRI. Neuroimage 31:496–504.

Wechsler D (2000): WAIS-III Echelle d'intelligence de Wechsler pour adultes. ECPA, Troisième Edition. Paris.

Wechsler D (2001): MEM III, échelle clinique de mémoire. ECPA, Paris.

Wu X, Li R, Fleisher AS, Reiman EM, Guan X, Zhang Y, Chen K, Yao L (2011): Altered default mode network connectivity in Alzheimer's disease—A resting functional MRI and Bayesian network study. Hum Brain Mapp 32:1868–1881.

Zhou J, Greicius MD, Gennatas ED, Growdon ME, Jang JY, Rabinovici GD, Kramer JH, Weiner M, Miller BL, Seeley WW (2010): Divergent network connectivity changes in behavioural variant frontotemporal dementia and Alzheimer's disease. Brain 133(Pt 5):1352–1367.